

1 Genome-wide analysis identifies a distinct pathophysiology for chronic  
2 overlapping pain conditions via impaired axonogenesis in the brain  
3

4 Samar Khoury<sup>1,†</sup>, Marc Parisien<sup>1,†</sup>, Scott J. Thompson<sup>1,2</sup>, Etienne Vachon-Presseau<sup>1</sup>, Mathieu  
5 Roy<sup>1,3</sup>, Amy E. Martinsen<sup>4,5,6</sup>, Bendik S. Winsvold<sup>4,5,7</sup>, the HUNT All-In PAIN group<sup>8</sup>, Ingunn  
6 Mundal<sup>9</sup>, John-Anker Zwart<sup>4,5,6</sup>, Artur Kania<sup>10</sup>, Jeffrey S. Mogil<sup>1,3</sup>, Luda Diatchenko<sup>1,\*</sup>

7  
8 1 Alan Edwards Centre for Research on Pain; Faculty of Dentistry; Department of Anesthesia,  
9 Faculty of Medicine, McGill University, Montréal, QC, Canada

10 † Equally contributing authors

11 2 Department of Anesthesiology, University of Minnesota, Minneapolis, MN USA

12 3 Department of Psychology, McGill University, Montréal, QC, Canada

13 4 K. G. Jebsen Center for Genetic Epidemiology, Department of Public Health and Nursing,  
14 Faculty of Medicine and Health Sciences, Norwegian University of Science and Technology,  
15 Trondheim, Norway

16 5 Department of Research, Innovation and Education, Division of Clinical Neuroscience, Oslo  
17 University Hospital, Oslo, Norway

18 6 Institute of Clinical Medicine, Faculty of Medicine, University of Oslo, Oslo, Norway

19 7 Department of Neurology, Oslo University Hospital, Oslo, Norway

20 8 HUNT All-In Pain Consortium

21 9 Department of Health Science, Molde University College, Molde, Norway

22 10 Institut de recherches cliniques de Montréal (IRCM); Department of Cell Biology and  
23 Anatomy, and Experimental Medicine, McGill University, Montréal, QC, Canada

24  
25 \* Corresponding author:

26 Professor Luda Diatchenko, MD, PhD

27 Faculty of Dentistry

28 Department of Anesthesia, Faculty of Medicine

29 McGill University

30 Genome Building, Room 2201

31 740 Dr. Penfield Avenue

32 Montreal, Quebec, Canada H3A 0G1

33 T: 514 398-2878 F: 514 398-8900

34 **ABSTRACT**

35 Chronic pain is often present at more than one anatomical location, leading to chronic  
36 overlapping pain conditions (COPC). Whether COPC represents a distinct pathophysiology from  
37 the occurrence of pain at only one site is unknown. Using genome-wide approaches, we  
38 compared genetic determinants of chronic single-site vs. multi-site pain in the UK Biobank. We  
39 found that different genetic signals underlie chronic single-site and multi-site pain with much  
40 stronger genetic contributions for the latter. Among 23 loci associated with multi-site pain, 9 loci  
41 replicated in the HUNT cohort, with the DCC netrin-1 receptor (*DCC*) as the top gene.  
42 Functional genomics identified axonogenesis in brain tissues as the major contributing pathway  
43 to chronic multi-site pain. Finally, multimodal structural brain imaging analysis showed that  
44 *DCC* is most strongly expressed in subcortical limbic regions and is associated with alterations in  
45 the uncinate fasciculus microstructure, suggesting that DCC-dependent axonogenesis may  
46 contribute to COPC via cortico-limbic circuits.

47

48

49

50 Chronic pain is a common and complex disease with a prevalence of 10–50% worldwide and is  
51 associated with substantial costs to affected individuals and society at large<sup>1-3</sup>. The clinical  
52 assessment of most chronic pain conditions relies on self-report of symptoms associated with a  
53 specific anatomical location. However, at least one-third of chronic pain patients diagnosed with  
54 one pain condition often simultaneously exhibit symptoms of another<sup>4,5</sup>. Epidemiological studies  
55 have examined the overlap between different bodily distribution of pain and suggested that they  
56 may share a common underlying etiology<sup>5</sup>. In these pain conditions, recently referred to as  
57 nociplastic, altered network architecture of functional brain connectivity seems to contribute to  
58 central sensitization and co-occurring symptoms include fatigue, mood and cognitive problems,  
59 sleep disturbances, and multisensory hypersensitivity<sup>6</sup>. The most common set of pain disorders  
60 that tend to overlap includes temporomandibular disorders, fibromyalgia, irritable bowel  
61 syndrome, vulvodynia, myalgic encephalomyelitis/chronic fatigue syndrome, headaches, and  
62 chronic lower back pain. This manifestation of multiple chronic pain conditions that frequently  
63 occur together and are associated with similar risk factors are referred to as chronic overlapping  
64 pain conditions (COPC), and are now recognized by the National Institute for Health (NIH) as a  
65 set of disorders that co-occur<sup>7</sup>. Although the pathophysiological processes that underlie most of  
66 these conditions are still poorly understood, COPC have been proposed to have common genetic,  
67 neurological, and psychological vulnerabilities.

68 Twin studies have indicated that chronic pain conditions show a heritability between 16–  
69 50%<sup>8</sup>. Shared heritability between pelvic pain and facial pain, and between widespread pain and  
70 abdominal pain have been reported<sup>9,10</sup>. Candidate gene studies have suggested that the same  
71 genetic variants are associated with multiple pain conditions, which implicated a possible shared  
72 genetic basis<sup>11</sup>. There remains a paucity of genetic findings based on genome-wide association

73 studies (GWAS) in large cohorts that have systematically assessed multiple chronic pain  
74 conditions. To date, most genetic association studies of pain have featured small samples of a  
75 single pain condition, with a few exceptions for back pain and multi-site pain<sup>12,13</sup>. It is still  
76 unknown whether the reports of COPC versus one specific chronic pain condition feature distinct  
77 pathophysiologies or are simply a manifestation of one another.

78 In this study, we employed genome-wide and brain structure analysis to understand the  
79 pathophysiology of COPC. Our first objective was to understand the genetic basis of chronic  
80 pain manifestation at one body site versus multiple body sites as a proxy for COPC. Our second  
81 objective was to uncover the molecular pathophysiology underlying COPC. Our final objective  
82 was to investigate whether central nervous system (CNS) mechanisms are genetically related to  
83 COPC. Our goal was to uncover the shared genetic heritability between chronic pain conditions  
84 and to search for potential underlying biological pathways for COPC.

85

## 86 **RESULTS**

### 87 **Prevalence of chronic pain sites**

88 In the UK Biobank, 294,627 participants (60%) reported pain that interfered with their usual  
89 activities in the past month. Participants were given the choice among eight pain sites, with the  
90 possibility to report more than one site (Figure 1A): head, facial, neck/shoulder, back,  
91 stomach/abdominal, hip, knee, and “all over the body”. The highest prevalence reported was for  
92 back (26%) and neck/shoulder (23%) pains. These participants were then asked if their pain  
93 lasted for more than three months. Participants who answered “yes” for pain that lasted for more  
94 than three months were classified as having chronic pain. Participants reported chronic pain for  
95 at least one site at 72%. The highest prevalence of chronic pain was reported for back (18%),  
96 knee (17%), and neck (16%) pains. Headache (9%), hip (9%), and abdominal (5%) pains showed  
97 less than 10% prevalence. Pain all over the body (1%) and facial pain (1%) displayed the lowest  
98 prevalence. Participants that reported pain in the last month and for more than three months at  
99 the same site, were defined as having pain chronification. Pain all over the body, knee, and hip  
100 pains showed the highest rates of chronification (81%, 78%, and 77%, respectively;  
101 Supplementary Table 1).

102 Next, we created two distinct groups to represent participants who reported only one  
103 chronic pain site and those who reported pain at two or more pain sites, which include  
104 participants with pain all over the body. We defined participants who reported more than one  
105 pain site for more than three months as participants with multi-site pain as a proxy for COPC.  
106 One third (34.1%) of participants with chronic pain reported multi-site pain and 38% reported  
107 single-site pain. Around 28% of participants did not report any chronic pain site (Supplementary  
108 Figure 1). In participants with multi-site pain, the highest odds ratio (OR) for pain at two sites

109 was for facial pain and headache (OR [95%CI] =10.7 [10.1-11.5]), followed by back and hip  
110 pain (OR [95%CI] =5.9 [5.8-6.1]) (Figure 1B, Supplementary Table 2). Pain all over the body  
111 was excluded from this analysis because participants who indicated pain all over the body did  
112 not have the option to report any other pain site. Participants who reported multi-site pain were  
113 more likely to be older, female, have higher body mass index, and have lower socioeconomic  
114 status. They were also more likely to report more cancer and non-cancer illnesses and to  
115 consume more paracetamol and ibuprofen, but not aspirin. In terms of mental health status,  
116 participants with multi-site pain reported higher neuroticism scores, and a higher number of and  
117 more severe depressive episodes (Table 1).

### 118 **Genetic correlation of chronic pain sites**

119 Most chronic pain sites were found to be genetically correlated (Figure 1B, Supplementary Table  
120 3). The largest genetic correlation was observed between facial and abdominal pain ( $r_g = 1.04$ ,  
121  $P=1.8 \times 10^{-10}$ ), followed by pain all over the body and abdominal pain ( $r_g = 0.99$ ,  $P=8.2 \times 10^{-8}$ ).  
122 Headaches presented the smallest genetic correlations with any other chronic pain sites ( $r_g$   
123 between 0.37 and 0.54). In a latent causal variable analysis to infer causality, we detected  
124 evidence for genetically causal effect of facial pain on hip pain. We also detected a genetic  
125 causal effect of headache on back, knee and neck/shoulder pains (Supplementary Table 4).

126 Pain site pairs that are physically close displayed stronger correlations (Figure 1B). Close  
127 physical proximity between two pain sites yields an increased chance of their being reported  
128 together (% variance explained:  $r^2=54\%$ ,  $P=1.4 \times 10^{-4}$ ) (Figure 1C). Also, increased genetic  
129 correlation is observed with close physical proximity ( $r^2=15\%$ ,  $P=4.9 \times 10^{-2}$ ) (Figure 1D). Genetic  
130 and epidemiological variables (pain sites) were also observed to be correlated ( $r^2=16\%$ ,  
131  $P=4.7 \times 10^{-2}$ ) (Figure 1E).

132 **Heritability of chronic pain sites**

133 For each chronic pain site, we calculated the heritability derived from genome-wide association  
134 ( $h^2_g$ ), defined as the proportion of phenotypic variance explained by common single nucleotide  
135 polymorphisms (SNPs) under an additive model of inheritance. Between 1–10% of the  
136 heritability can be explained for each pain site (Figure 1F, Supplementary Table 5). The highest  
137 heritability was identified for back pain ( $h^2_g=10.0\%$ ,  $P=7\times 10^{-106}$ ) while the lowest was for facial  
138 pain ( $h^2_g=1.4\%$ ,  $P=1\times 10^{-5}$ ).

139 **Genome-wide associations of chronic overlapping pain conditions**

140 Next, we performed a comparative GWAS analysis for the report of chronic single-site pain with  
141 the report of chronic multi-site pain. In a total sample of 340,547 participants we conducted a  
142 GWAS contrasting the report of one pain site ( $n=93,964$ ) with a randomly selected half of  
143 participants who reported no pain at any site ( $n=81,805$ ). We also conducted a GWAS  
144 contrasting the report of multi-site ( $n=82,812$ ) with non-overlapping controls as the rest of the  
145 randomly selected participants who reported no pain at any site ( $n=81,966$ ).

146 We then computed the percentage of variance explained by genetic and by environmental  
147 factors for the report of single-site versus multi-site pain. We found a substantial contribution of  
148 environmental factors for both the report of single-site (93.2%; standard error of the mean  
149 (s.e.m) 0.4%) and multi-site (80.9%; s.e.m 0.4%) pain. However, we found a significant  
150 difference ( $P<2.2\times 10^{-16}$ ) for genetic factors between the report of single- site pain (6.9%;  
151 s.e.m.0.4%) and the report of multi-site pain (19.1%; s.e.m 0.4), with a much greater genetic  
152 contribution in chronic multi-site pain (Figure 1F). Importantly, the heritability for multi-site  
153 pain was twice higher than heritability for any individual pain site.

154 In the case-control association study, where cases were defined as participants reporting  
155 chronic single-site pain (n=93,964), and controls being participants not reporting any pain site  
156 (n=81,805), there were no individual loci that passed the threshold of genome-wide significance  
157 (Figure 2A, Supplementary Table 6). The genomic inflation factor lambda was 1.07, but the LD  
158 score regression intercept value was 1.015, suggesting a polygenic signal rather than inflation  
159 from unaccounted population stratification (Supplementary Figure 2A). A gene-level association  
160 analysis in MAGMA testing for 18,220 genes showed that 11 genes passed multiple testing  
161 (Bonferroni threshold  $P < 2.7 \times 10^{-6}$ ) (Supplementary Table 7).

162 In the case-control genome-wide association study, where cases were defined as  
163 participants reporting chronic multi-site pain (n=82,812), and controls being participants not  
164 reporting any pain site (n=81,966), there were 896 SNPs spanning 23 loci that passed the  
165 genome-wide threshold (Figure 2B, Supplementary Figure 3, Supplementary Table 8). The  
166 genomic inflation factor lambda was 1.20, but the LD score regression intercept value was 1.017,  
167 suggesting again, a contribution of LD structure of associated loci rather than inflation from  
168 unaccounted-for population stratification (Supplementary Figure 2B). A gene-level analysis  
169 showed that 97 genes passed multiple testing ( $P = 2.7 \times 10^{-6}$ ). The two top associations were with  
170 genes involved in neuronal connectivity in model animals: *DCC*<sup>14</sup>, encoding the DCC receptor  
171 for netrin1 ( $P = 7.4 \times 10^{-19}$ ), and *SDK1*<sup>15</sup>, encoding the sidekick cell adhesion molecule 1  
172 ( $P = 5.4 \times 10^{-18}$ ) (Supplementary Table 9). Since both GWASs were equally powered, the  
173 differences observed at both the SNP and the gene-level analyses might partially account for the  
174 differences in heritability estimates, establishing distinct genetic backgrounds.

## 175 **Genome-wide meta-analysis**



176 In order to identify loci that were specific to individual pain states (i.e., single-site and  
177 multi-site pain) and pleiotropic loci that contribute to both states, we performed two meta-  
178 analyses using GWAMA<sup>16</sup>. The first meta-analysis aimed to identify loci that are distinct for  
179 each of the GWASs (Figure 2C). Out of the 18,066 genes tested, 41 genes passed the threshold  
180 for multiple testing (Supplementary Table 10). The top two genes shown in the meta-analysis are  
181 *DCC* and *SDK1*, which are also the top two genes in chronic multi-site pain. The second meta-  
182 analysis aimed to identify loci that are pleiotropic between the report of single-site pain and  
183 multi-site pain by running a classical fixed-effect meta-analysis between the two GWASs (Figure  
184 2D). There are 36 genes that passed the threshold for multiple testing, with the top two genes  
185 being *BBX* and *PABPC4* (Supplementary Table 11). Overall, we found that there are both  
186 distinct and common genetic loci underlying chronic single-site pain and chronic multi-site pain.

#### 187 **Tissue-expression based functional analyses**

188 Next, we performed partitioned heritability analyses by means of a stratified LD score  
189 regression<sup>17,18</sup> to examine whether the observed heritability was enriched in any tissue,  
190 regulatory region or functional category<sup>19</sup>. Analyses in a wide range of tissues and cell types<sup>20</sup>  
191 were done for both the report of single-site pain and multi-site pain. Partitioned heritability  
192 analysis for single-site pain did not show any enrichment in any of the tested tissues at a 10%  
193 false discovery rate (FDR) (Figure 3A – Top panel, Supplementary Table 12). The analysis of a  
194 wide range of tissues and cell types for chronic multi-site pain yielded significant results  
195 exclusively in the CNS, but not in other tissue types like adipose, blood or immune, and  
196 connective or musculoskeletal, nor in the peripheral nervous system (Figure 3A – Bottom panel,  
197 Supplementary Table 13). We found an exclusive significant enrichment in most brain tissues  
198 (Figure 3B). Finally, in order to quantify whether the enrichment was exclusive to multi-site

199 pain, we correlated the heritability estimates in brain-specific tissues. We found no evidence for  
200 tissue-based congruency between the two heritability estimates, which suggests distinct tissue  
201 heritability (Figure 3C). Tissue-expression based analysis concluded that heritability for chronic  
202 multi-site pain, and not chronic single-site pain, is exclusively enriched in the CNS.

### 203 **Pathway-based functional analyses**

204 We next performed pathway-based enrichment analyses from SNPs in gene sets using Gene  
205 Ontology's (GO) biological processes for both chronic single-site pain and multi-site pain. For  
206 the report of chronic single-site pain, there was no enrichment in any pathway at FDR 10% in  
207 GO biological process (Supplementary Table 14). For the report of chronic multi-site pain, a  
208 total of 60 pathways were significant at the FDR 10% level in GO biological process, with most  
209 pathways involved in neural development, that include *DCC* and *SDK1* as leading-edge genes  
210 (Supplementary Table 15). We then used *reviGO*<sup>21</sup> to reduce redundancy and extricate  
211 meaningful information regarding biological processes. The top *reviGO* class of pathway  
212 identified regulation of nervous system development that encompasses pathways involving  
213 neurogenesis, axonal development and post-synaptic specialization. Taken altogether, our  
214 pathway analysis results were in line with tissue-expression based functional analysis suggesting  
215 that pathways acting in the CNS in general and associated with neural development in particular,  
216 contribute to the pathophysiology of chronic multi-site pain. Moreover, pathway analysis further  
217 supported a strong genetic basis for chronic multi-site pain but not for chronic single-site pain.

### 218 **Replication of genome-wide loci in an independent cohort**

219 Next, we attempted to replicate the genome-wide significant SNPs in the independent HUNT  
220 cohort. Due to the absence of genome-wide significant SNPs in the chronic single-site pain  
221 GWAS, we only replicated the chronic multi-site pain variants. We attempted the replication of

222 the lead SNP in each of the loci and for SNPs that are in medium ( $r^2 \geq 0.5$ ) and high LD  
223 ( $r^2 \geq 0.8$ ) with it in the HUNT cohort. Out of the 23 loci, nine loci reached nominal significance  
224 at  $P \leq 0.05$ , of which four reached statistical significance at  $P \leq 0.002$  (corrected for 23 tests)  
225 (Supplementary Table 16). The following four loci passed the threshold for multiple testing.  
226 Locus 4, with lead SNP rs11709734, located on chromosome 3 in the inositol  
227 hexakisphosphate kinase 1 (*IP6K1*) gene. Locus 8, with lead SNP rs34595097, located on  
228 chromosome 4 in the mastermind like transcriptional coactivator 3 (*MAML3*) gene. Locus 11,  
229 with lead SNP rs12672683, located on chromosome 7 in the forkhead box P2 (*FOXP2*) gene.  
230 Finally, locus 20, with lead SNP rs8099145, located on chromosome 18 in the *DCC* gene,  
231 showed the most robust replication ( $P=2.0 \times 10^{-4}$ ) (Table 2a).

232 Next, we attempted to replicate the 97 genes associated with chronic multi-site pain in the  
233 UK Biobank within the HUNT cohort. The threshold for replication was corrected for 97 tests  
234 and set at  $P=5.6 \times 10^{-4}$ . Out of the 97 genes, 11 genes successfully replicated. The most striking  
235 association is with the *DCC* gene with a p-value of  $2.6 \times 10^{-8}$ , reaching genome-wide statistical  
236 significance (Supplementary Table 16, Table 2).

237 Finally, at the pathway level, we attempted to replicate the pathways that passed FDR  
238 10% in the UK Biobank. The axonogenesis pathway (GO:0007409) showed the lowest  $P$ -value  
239 in the HUNT cohort. This pathway represents mechanisms involved in *do novo* generation of  
240 axons, including the terminal branched region. This morphogenesis also includes the shape and  
241 form of the developing axon. The second pathway was axon development (GO:0061564), which  
242 covers processes that involve axon regeneration or regrowth after loss or damage  
243 (Supplementary Table 16, Table 2).

244 In summary, the replication of our results in HUNT cohort provided further evidence that  
245 axonogenesis through the netrin receptor DCC is important in the pathophysiology of chronic  
246 multi-site pain.

### 247 **Functional validation for the role of *DCC* in the human brain**

248 Chronic multi-site pain-related heritability seems to be expressed in brain tissues with a  
249 significant role for the axonogenesis pathway through the *DCC* gene. We therefore attempted to  
250 localize where *DCC* is most strongly expressed using a fine-grained representation of genomic  
251 information across the human brain and identify the location of axonal structures using diffusion  
252 weighted imaging.

253 First, normalized *DCC* expression information was obtained from approximately 500  
254 brain samples (per hemisphere) of six deceased human donors from the Allen Human Brain  
255 Atlas<sup>22</sup>. A heat map representing the normalized *DCC* expression across the donors was  
256 generated using the neurosynth platform. We observed that *DCC* is specifically expressed in  
257 subcortical limbic regions, such as the hippocampus, and basal ganglia (Figure 4A-B), the  
258 corticolimbic system involved in motivation and affect regulation as well as the amplification  
259 and the chronification of pain.

260 Given our findings on the role of *DCC*-driven axonogenesis in chronic multi-site pain  
261 and *DCC* expression in corticolimbic circuits, we next examined the associations between the  
262 microstructure of the uncinate fasciculus (UF) which connects the prefrontal cortex to limbic  
263 structures of the temporal lobe such as the amygdala and the hippocampus (Figure 4C). The UF  
264 is also the main cortico-limbic tract available as an imaging derived phenotype (IDP) in the UK  
265 Biobank. Analyses of the UF were performed on 5378 participants that consistently reported no

266 pain (n=3,985), single-site pain (n=593), or multi-site pain (n=800) on both the initial visit and  
267 the brain imaging visit (about 10 years apart). Orientation dispersion (OD), a spatial organization  
268 metric that characterizes angular variation of neurites (dendrites and axons), was extracted as a  
269 metric with potential relevance to axon guidance for the left and the right uncinate fasciculus and  
270 was compared between the groups. Our analysis revealed that participants with multi-site pain  
271 showed significantly higher OD in UF compared to single-site pain and healthy controls (Figure  
272 4D), indicating that UF white matter tracts in patients with COPC are less structured.

273 In order to assess whether genetic variants in *DCC* and axonogenesis pathway contribute  
274 to the OD of the UF, we generated a polygenic risk score (PRS) using summary statistics of  
275 single-site pain, multi-site pain, the axonogenesis pathway, and the *DCC* gene using the best  
276 PRS, i.e. which explains the highest variance. Each of the four scores were used as dependent  
277 variables in a regression model with left and right OD of the UF as independent variable  
278 (Supplementary Table 17). The score generated using *DCC* showed the highest significance for  
279 both brain sides OD of the UF. The PRS derived from the single-site GWAS at a *P*-value  
280 threshold of  $5 \times 10^{-8}$  explained 0.034-0.044% of the variability ( $P=1.0 \times 10^{-5}$ ;  $P=5.5 \times 10^{-4}$ ) for the  
281 left and right UF respectively. PRS derived from the multi-site pain GWAS at a *P*-value  
282 threshold of  $4 \times 10^{-2}$  explained 0.035% and 0.029% of the variability ( $P=4.8 \times 10^{-4}$ ;  $P=1.4 \times 10^{-3}$ ) for  
283 the left and right UF respectively. PRS derived from the axonogenesis pathway at a *P*-value  
284 threshold of  $5.5 \times 10^{-2}$  explained 0.017% of the variability ( $P=1.6 \times 10^{-2}$ ) for both left and right UF.  
285 PRS derived from the *DCC* gene at a *p*-value threshold of  $7 \times 10^{-2}$  explained 0.05% of the  
286 variability ( $P=2.5 \times 10^{-5}$ ;  $P=1.3 \times 10^{-4}$ ) for the left and right UF respectively (Figure 4E). Overall,  
287 our results showed that the UF is an important structure contributing to pain and especially

288 multi-site pain through *DCC*, bridging together for the first-time the genetic determinants of  
289 COPC with corticolimbic structures of the human brain.

290 **DISCUSSION**

291 The propensity of chronic pain patients to report more than one location of chronic pain is often  
292 observed in clinical settings. Patients diagnosed with one chronic pain condition, such as  
293 fibromyalgia, temporomandibular disorder, or headaches, have higher chances of presenting  
294 symptoms of other pain conditions<sup>4,5</sup>. Moreover, these patients also report comorbid symptoms  
295 such as sleep disturbances, depression, and anxiety<sup>23-25</sup>. Whether COPC is a distinct  
296 pathophysiology from the occurrence of single-site chronic pain is unknown<sup>5</sup>.

297 Our analysis of the UK Biobank, one of the largest available datasets, confirmed the high  
298 degree of overlap between different chronic pain sites, with one-third of participants with chronic  
299 pain reporting multiple pain sites, another third reporting only one pain site, and the remaining  
300 third reporting no pain. Our GWAS results showed that distinct genetic factors underlie the  
301 report of a single pain condition versus the report of COPC, with multi-site pain having a much  
302 stronger genetic component than single-site pain. Furthermore, our study identified a genetic  
303 correlation between different chronic pain sites derived from genome-wide data. The strong  
304 genetic correlation between chronic pain sites and the causal latent analysis suggests that there is  
305 a specific pathway of vulnerability that underlies co-occurring pain conditions, confirming  
306 previous observations of twin studies<sup>9</sup>. Headaches, although also highly heritable, did not show  
307 genetic overlap with other chronic pain sites, which suggests a distinct pathophysiology. Indeed,  
308 previous GWASs of headaches and migraines have shown a strong cardiovascular component<sup>26</sup>,  
309 whereas in this paper we demonstrated a substantial involvement of CNS components in the  
310 genetic pathophysiology of COPCs. Finally, we also confirmed the results of a previous twin  
311 study demonstrating a high genetic correlation between widespread pain and abdominal pain<sup>9</sup>.

312 In the field of pain, the majority of existing genetic findings are derived from candidate  
313 gene approaches related to specific pain conditions<sup>11,27</sup>. Only recently have large genome-wide  
314 studies started to emerge from the UK Biobank for migraine, back pain, as well as multi-site  
315 pain, where investigators found many of the SNPs that we uncovered as well<sup>12,13,28</sup>. Here, we  
316 aimed to identify the genetic architecture and associated biological pathways of COPC rather  
317 than any specific SNP for a specific pain condition and discovered more than 900 variants  
318 associated with COPC. These genetic factors explain up to 20% of the variance for multi-site  
319 pain, while the heritability for any individual pain site was lower, suggesting a much stronger  
320 genetic basis for COPC in comparison with single pain conditions. When we compared the  
321 genetic relationship between the report of chronic single-site pain and chronic multi-site pain, we  
322 find both common and distinct loci. Contrary to the report of single-site pain, COPC is highly  
323 polygenic, with a large portion of its heritability conferred by common genetic variants. The loci  
324 that are specific to COPC are enriched in the CNS and are involved in mechanisms related to  
325 axonogenesis with a leading role for the *DCC* gene. While the previous studies have found an  
326 association between SNPs in *DCC* locus and pain, among many others<sup>12,13</sup> our approaches took  
327 single SNP associations results further and identified the central role of *DCC* in the genetics of  
328 COPC and uncovered corresponding functional role for netrin and its receptor in the human brain  
329 contributing to COPC pathophysiology. Importantly, we also replicated our human findings in  
330 another large and independent cohort.

331 Axon guidance is a process by which neuronal growth cones guide axon extension in the  
332 developing nervous system<sup>29</sup>. It involves molecular cues such as netrin 1, present in the  
333 environment of growth cones, signaling via dedicated receptors, such as DCC, expressed on the  
334 surface of growth cones<sup>14,30-33</sup>. Interestingly, changes in netrin 1 dependent peripheral nerve



335 outgrowth have been reported in patients with chronic pain<sup>30,34</sup>, suggesting that netrin may  
336 continue to play an important role following nervous system assembly. The results of the present  
337 study further demonstrate that cerebral axonogenesis contributes to COPC. First, heritability  
338 partitioning analyses clearly indicated that heritability for multi-site pain was related to genes  
339 expressed in the brain. Second, brain imaging data from the Allen Brain Atlas and UK Biobank  
340 pointed towards corticolimbic circuits with the UF as a candidate structure for explaining the  
341 relationship between the *DCC* gene and COPC.

342 More specifically, *DCC* gene expression in the human brain appears to be remarkably  
343 circumscribed within the basal ganglia and hippocampus. In addition, structural connectivity of  
344 the UF was also found to be related to both the *DCC* gene and to multi-site pain. Increased OD  
345 values in the UF for multi-site pain suggests that white matter tracts in the UF are less structured  
346 in patients exhibiting multi-site pain. This finding seems to be highly consistent with the role of  
347 the UF in emotional regulation. The UF, which develops well into the fourth decade of life,  
348 connects the medial and lateral orbitofrontal cortex with limbic structures in the temporal lobe  
349 such as the amygdala and parahippocampal gyrus<sup>35</sup>. One of the main functions of the UF is to  
350 provide subcortical structures with contextual information about potential threats and reward  
351 available in the orbitofrontal cortex. As such, UF anatomy has been related to general deficits in  
352 the capacity to flexibly predict rewards and punishments, as well as to various neuropsychiatric  
353 disorders characterized by emotional dysregulation and poor impulse control, such as major  
354 depressive disorder (MDD), attention deficit/hyperactivity disorder (ADHD) and drug abuse<sup>35</sup>.

355 Interestingly, previous studies have shown that the *DCC* gene orchestrates the  
356 development of the prefrontal cortex during adolescence<sup>36</sup>. Moreover, GWASs of the UK  
357 Biobank have also associated the *DCC* gene with neuropsychiatric disorders characterized by

358 mood instability such as MDD, post-traumatic stress disorder (PTSD), bipolar disorder (BD), or  
359 ADHD<sup>37,38</sup>.

360 Our findings add to these results by linking *DCC* with disorganization of the UF and  
361 multi-site pain. Here, we showed that participants who report COPC have higher disorganization  
362 in axonal tracks versus participants that report only one pain site or healthy participants. This  
363 finding suggests that rewiring of the developing brain predispose to the development of chronic  
364 pain. A PRS analysis shed the light on a potential relationship between white matter tract  
365 organization in the brain and COPC and showed that variants belonging to *DCC* gene are  
366 important mediators of this relationship.

367 An exclusive involvement of the CNS in pathophysiology of COPC found in our study should be  
368 interpreted with caution. Our current results are limited by the broadness of the datasets we use.  
369 For instance, our partition heritability analyses did not identify expression from spinal cord,  
370 DRGs, or peripheral nerves contributing to multi-site pain. Yet, we are limited here in our  
371 analyses of the expression of adult tissues, when we know that *NTN1* and *DCC* are not expressed  
372 in the adult spinal cord but only during development. With the increasing broadness of the  
373 available expression datasets, new roles for *DCC* may be discovered in addition to that identified  
374 here: its crucial contribution to COPC through the wiring of the CNS.

375 In conclusion, we identified a unique and distinct genetic basis for chronic overlapping  
376 pain conditions that points to netrin-driven axonogenesis. Our results suggest that genetically  
377 determined *DCC*-dependent axonogenesis in the UF microstructure contributes to COPC via  
378 corticolimbic circuits. CNS mechanisms, whether overlapping or distinct, have been suggested as  
379 a common neurobiological substrate that may underlie the development of COPC<sup>5,39</sup>. Here, we

380 identified the genetic and structural basis of this CNS input. Thus, our results suggest a new  
381 direction in both fundamental research and therapeutics development.

382

383

384 **ONLINE METHODS**

385 **Study cohort – UK Biobank**

386 The UK Biobank is a large, prospective, multicenter study of the United Kingdom’s population  
387 recruited between 2006 and 2010<sup>40,41</sup>. Participants were 40–69 years old and lived within 25  
388 miles of a study recruitment center. Chronic pain conditions were assessed for 502,599  
389 individuals at the initial assessment visit (2006-2010) using a touchscreen-based question: “In  
390 the last month, have you experienced any of the following that interfered with your usual  
391 activities?” (Data field 6159). The participants had a choice between pain all over the body, back  
392 pain, facial pain, headaches, knee pain, stomach/abdominal pain, hip pain, neck/shoulder pain,  
393 none of the above and prefer not to answer. For each pain site selected, participants were asked if  
394 that pain lasted for more than 3 months (Data fields 2956: pain all over the body; 3404:  
395 neck/shoulder pain; 3414: hip pain; 3571: back pain; 3741: stomach/abdominal pain; 3773: knee  
396 pain; 3799: headaches; 4067: facial pain). Participants that answered pain all over the body could  
397 not indicate any other body site. Cases were defined as individuals self-reporting pain that  
398 interfered with their usual activities in the last month and/or that had lasted for more than 3  
399 months. Participants that reported pain at one month and at three months at the same site were  
400 defined as having pain chronification. Controls were defined as the participants that answered  
401 “none of the above” to data field 6159. Participants that answered, “prefer not to answer” and  
402 “do not know” were excluded. Of the 502,599 individuals, 404,381 had phenotype and genotype  
403 data available and therefore were analyzed in this paper.

404 **Statistical analysis**

405 Statistical analyses were done using SPSS IBM v 22.0. The prevalence of each chronic pain  
406 condition was assessed. The odds ratio (OR) and 95% confidence interval (95% CI) were

407 calculated to quantify the degree of overlap between conditions. Next, we classified the study  
408 population in two groups. The first group included individuals that reported only one pain site  
409 that lasted for more than 3 months. The second group included individuals that reported more  
410 than one pain site that lasted for more than 3 months, including those who reported widespread  
411 pain. This second group was defined as cases reporting multi-site pain as a proxy for chronic  
412 overlapping pain conditions (COPC).

### 413 **Genetic analysis**

414 Out of the 404,381 participants that underwent genotyping and that have available phenotype  
415 information, we excluded participants that were not genetically confirmed as “white British”,  
416 that had sex aneuploidy, or that have a high ( $\geq 2\%$ ) genotypic missingness rate. After quality  
417 control filters were applied, 340,547 participants were considered for analysis. We conducted  
418 eight genome-wide association studies (GWASs), one for each pain site, using a logistic  
419 regression model to assess heritability and genetic correlations. Next, we also conducted a  
420 GWAS contrasting the report of one pain site ( $n=93,964$ ) with a randomly selected half of  
421 participants that answered “none of the above” to data field 6159 ( $n=81,805$ ). We also conducted  
422 a GWAS for chronic multi-site pain, with cases defined as individuals reporting more than one  
423 pain site ( $n=82,812$ ) and controls as the rest of the randomly selected participants that answered  
424 “none of the above” to data field 6159 ( $n=81,966$ ). All genetic analyses were conducted using a  
425 logistic regression model with the following co-variates: 40 principle components to account for  
426 population stratification, age, age<sup>2</sup>, sex, genotyping array, and dummy coded recruitment sites.  
427 BOLT-LMM v.2.3 was used in all GWAS analyses, as it accounts for cryptic relatedness<sup>42</sup>.  
428 Autosomal analysis was restricted to variants with a MAF  $>0.1\%$ , info score  $>0.8$ , genotype hard  
429 call rate  $>0.95$ , and Hardy–Weinberg  $P >1 \times 10^{-12}$ . A total of 8,239,177 autosomal makers with

430 minor allele frequencies above 0.1% that passed quality controls were tested. Heritability was  
431 estimated from single nucleotide polymorphisms (SNPs) under an additive model of inheritance  
432 using BOLT-REML<sup>42</sup> and LD Score Regression (LDSC)<sup>43</sup>.

433 Genetic correlations were estimated for each pair of pain conditions using LDSC<sup>44</sup>.  
434 Tissue-based partitioned heritability was evaluated using LD Score Regression<sup>17,18</sup>, with the  
435 dataset from the Xavier lab<sup>19</sup>.

#### 436 **Gene-based analysis**

437 Gene-based analysis was done using MAGMA. SNPs derived from the summary GWAS were  
438 mapped to 18,714 protein-coding genes. A threshold of genome-wide significance level was  
439 estimated at  $P < 2.67 \times 10^{-6}$ .

#### 440 **Genome-wide meta-analysis**

441 In order to identify shared and unique genetic loci between single and multi-site chronic pain  
442 summary GWAS datasets, a meta-analysis was performed using GWAMA<sup>16</sup> that was adapted  
443 from the sex-specific analysis described previously<sup>45</sup>. The code was adapted to replace the “sex-  
444 differentiated” option where we assigned “males” as single-site pain and “females” as multi-site  
445 pain<sup>45</sup>. The results of GWAMA will show unique and pleiotropic loci.

#### 446 **Functional mapping and annotation**

447 We used the online platform of FUMA<sup>46</sup> v.1.3.4 to obtain comprehensive annotation information  
448 from GWAS summary data. Gene-based tests were obtained using MAGMA<sup>47</sup>.

449 Pathway analyses were conducted with MAGMA within Gene Ontology’s (GO) biological  
450 processes<sup>48</sup>. Reduction and visualization of GO pathways was done using revigo<sup>21</sup>.

#### 451 **Replication study cohort –HUNT**

452 *Participants in the HUNT Study*

453 The Nord-Trøndelag Health Study (HUNT) is an ongoing population-based cohort study from  
454 the county of Nord-Trøndelag in Norway<sup>49,50</sup>. All inhabitants aged 20 years or older were invited  
455 to participate in the HUNT1 survey (1984-1986), the HUNT2 survey (1995-1997), and the  
456 HUNT3 survey (2006-2008). Participation rates in HUNT1, HUNT2 and HUNT3 were 89.4%  
457 (n=77,212), 69.5% (n=65 237) and 54.1% (n=50 807), respectively<sup>50</sup>. Taken together, the study  
458 included more than 120,000 different individuals from Nord-Trøndelag County. For the present  
459 study, we included participants from HUNT2 and HUNT3. All participants have provided  
460 questionnaire, interview, and measurement data, which can be found at the HUNT databank  
461 [<https://hunt-db.medisin.ntnu.no/hunt-db>]. In addition, about 80,000 participants have provided  
462 biological samples for storage at the HUNT biobank [<https://www.ntnu.edu/hunt/hunt-biobank>].

#### 463 *Phenotype definition in HUNT*

464 The pain questionnaires in HUNT2 and HUNT3 have been described in detail previously<sup>51</sup>. In  
465 brief, participants who answered "yes" to the screening question “Have you during the last year  
466 continuously for at least 3 months had pain and/or stiffness in muscles and joints?” were  
467 requested to indicate the site of the pain, with the possibility to select one or more sites among  
468 the following: neck, shoulders, elbows, wrist/hands, upper back, low back, hips, knees, and/or  
469 ankles/feet. Cases with chronic multi-site pain were defined as those reporting pain at two or  
470 more sites. Controls were defined as those who answered "no" to the screening question on  
471 chronic pain. If an individual had participated in both HUNT2 and HUNT3, information from  
472 HUNT2 was used. This resulted in a total of 25,747 cases with multi-site pain and 35,753  
473 controls without chronic pain.

474

#### 475 *Genotyping, quality control and imputation*

476 In total, DNA from 71,860 HUNT samples was genotyped using one of three different Illumina  
477 HumanCoreExome arrays (HumanCoreExome12 v1.0, HumanCoreExome12 v1.1 and UM  
478 HUNT Biobank v1.0). Samples that failed to reach a 99% call rate, had contamination > 2.5% as  
479 estimated with BAF Regress<sup>52</sup>, large chromosomal copy number variants, lower call rate of a  
480 technical duplicate pair and twins, gonosomal constellations other than XX and XY, or whose  
481 inferred sex contradicted the reported gender, were excluded. Samples that passed quality control  
482 were analyzed in a second round of genotype calling following the Genome Studio quality  
483 control protocol described elsewhere<sup>53</sup>. Genomic position, strand orientation and the reference  
484 allele of genotyped variants were determined by aligning their probe sequences against the  
485 human genome (Genome Reference Consortium Human genome build 37 and revised  
486 Cambridge Reference Sequence of the human mitochondrial DNA; <http://genome.ucsc.edu>)  
487 using BLAT<sup>54</sup>. Variants were excluded if their probe sequences could not be perfectly mapped,  
488 cluster separation was < 0.3, Gentrain score < 0.15, showed deviations from Hardy Weinberg  
489 equilibrium in unrelated samples of European ancestry with p-value < 0.0001), had a call rate <  
490 99%, or another assay with higher call rate genotyped the same variant. Ancestry of all samples  
491 was inferred by projecting all genotyped samples into the space of the principal components of  
492 the Human Genome Diversity Project (HGDP) reference panel<sup>55,56</sup> (938 unrelated individuals;  
493 downloaded from <http://csg.sph.umich.edu/chaolong/LASER/>), using PLINK. Recent European  
494 ancestry was defined as samples that fell into an ellipsoid spanning exclusively European  
495 population of the HGDP panel. The different arrays were harmonized by reducing to a set of  
496 overlapping variants and excluding variants that showed frequency differences > 15% between  
497 data sets, or that were monomorphic in one and had MAF > 1% in another data set. The resulting  
498 genotype data were phased using Eagle2 v2.3<sup>57</sup>.



499 Imputation was performed on the 69,715 samples of recent European ancestry using  
500 Minimac3<sup>58</sup> (v2.0.1, <http://genome.sph.umich.edu/wiki/Minimac3>) with default settings (2.5 Mb  
501 reference based chunking with 500kb windows) and a customized Haplotype Reference  
502 consortium release 1.1 (HRC v1.1) for autosomal variants and HRC v1.1 for chromosome X  
503 variants<sup>59</sup>. The customized reference panel represented the merged panel of two reciprocally  
504 imputed reference panels: (1) 2,201 low-coverage whole-genome sequences samples from the  
505 HUNT study and (2) HRC v1.1 with 1,023 HUNT WGS samples removed before merging. We  
506 excluded imputed variants with Rsq < 0.3 or minor allele count < 3.

#### 507 *Association testing*

508 We used the Scalable and Accurate Implementation of GEneralized mixed model (SAIGE)<sup>60</sup>,  
509 which uses a generalized mixed model to account for sample relatedness and cryptic population  
510 structure. We ran a mixed logistic regression model, including sex, age, genotyping batch, and  
511 the first 4 principal components as covariates. The principal components were calculated by  
512 projecting all samples into the space of the principal components of unrelated HUNT samples,  
513 using directly genotyped variants in PLINK v1.90<sup>61</sup>.

#### 514 *Ethics*

515 The current study is approved by the Regional Committee for Medical and Health Research  
516 Ethics (ref. 2015/573).

#### 517 **Allen Brain Atlas**

518 Human gene expression data for visualization of *DCC* expression in the brain were obtained  
519 from the Allen Human Brain Atlas (<http://human.brain-map.org>). A detailed description of this  
520 dataset can be found elsewhere<sup>22</sup>. The Neurosynth platform (<https://neurosynth.org/>) was used  
521 extract heat map of normalized expression of *DCC* across the cerebral cortex and subcortical

522 regions. Visualization of the extracted heat map was done using either Brain Net Viewer<sup>62</sup> or  
523 MRICron (<https://www.nitrc.org/projects/mricron>).

#### 524 **Brain imaging in the UK Biobank**

525 Brain imaging occurred on a subset of subjects at a subsequent brain imaging visit. Inclusion into  
526 the pain groups therefore necessitated that subjects met the same chronic pain report on both the  
527 initial baseline visit and brain imaging visit. This resulted in 3,985 subjects with no pain, 593  
528 subjects with one-site pain and 800 subjects with multi-site pain. Here, we focused on  
529 diffusion-weighted imaging in the UF following the identification of the axonogenesis pathway  
530 and the expression of *DCC* in regions the corticolimbic system.

531 Diffusion data were acquired using a spin-echo echo-planar imaging sequence with two  
532 b-values ( $b = 1,000$  and  $2,000$  s/mm<sup>2</sup>) at 2-mm spatial resolution. The diffusion-weighted  
533 volumes were acquired with 100 distinct diffusion-encoding directions with multiband  
534 acceleration factor of 3. The field of view was  $104 \times 104$  mm, imaging matrix  $52 \times 52$ , 72 slices  
535 with slice thickness 2 mm, giving 2 mm isotropic voxels. Additional details about the sequence  
536 of acquisitions and extraction of IDPs in the UK Biobank can be obtained here:  
537 <https://biobank.ctsu.ox.ac.uk/crystal/refer.cgi?id=1977>. Briefly, the data was first corrected for  
538 eddy currents and head motion using the Eddy tool. Second, the tracts were derived using  
539 probabilistic tractography analysis (BEDPOSTx / PROBTRACKx). The automatic mapping of  
540 the 27 major white matter tracts was conducted in standard space of each participant using  
541 start/stop region of interest masks (implemented using the AutoPtx plugin for FSL). Maps of  
542 fractional anisotropy (FA), mean diffusivity (MD), intracellular volume fraction (ICVF),  
543 isotropic volume fraction (ISOVF) and orientation dispersion (OD) were registered with the  
544 AutoPtx tract masks, allowing the calculation of the averaged value for each parameter across all

545 voxels pertaining to each tract of interest. Here, we specifically focused on the angular variation  
546 in neurite orientation (OD) in the UF.

547         The OD of neurites can range from highly parallel (coherently oriented white matter  
548 structures, such as the corpus callosum) to highly dispersed (gray matter structures characterized  
549 by sprawling dendritic processes in all directions).

### 550 **Polygenic risk scores**

551 Polygenic risk scores (PRSs) were generated using PRSice v.2.3.3<sup>63</sup> using as a base summary  
552 GWAS results derived from the single-site and the multi-site GWAS by excluding participants  
553 with imaging results. PRSet was used to generate PRSs for the axonogenesis pathway  
554 (GO:0007409) and the *DCC* gene with 100 kb on each side. SNPs were clumped using the  
555 maximum haplotype frequency estimates and permutation was performed 10,000 times to  
556 generate an empirical *P*-values and to prevent Type 1 errors. A regression model that included  
557 sex, age, scan site and head scales were used as covariates in a model where each participant's  
558 PRS was the dependent variable. A PRS was generated for a series of *P*-value thresholds ( $5 \times 10^{-8}$ ,  
559  $1 \times 10^{-7}$ ,  $10^{-6}$ ,  $10^{-5}$ ,  $10^{-4}$ ,  $10^{-3}$ , 0.04, 0.05, 0.1, 0.2, 0.3, 0.4, 0.5, and 1) in the summary GWAS were  
560 to determine the association between pain-related genetic variants and left and right OD of the  
561 UF. The best-fit *P*-value threshold was used in the analysis.

562 **ACKNOWLEDGEMENTS**

563 This work was funded by the Canadian Excellence Research Chairs (CERC09). The current  
564 study was conducted under UK biobank application no. 20802. The Nord-Trøndelag Health  
565 Study (The HUNT Study) is a collaboration between HUNT Research Centre (Faculty of  
566 Medicine and Health Sciences, NTNU, Norwegian University of Science and Technology),  
567 Trøndelag County Council, Central Norway Regional Health Authority, and the Norwegian  
568 Institute of Public Health. The genotyping was financed by the National Institute of health  
569 (NIH), University of Michigan, The Norwegian Research council, and Central Norway Regional  
570 Health Authority and the Faculty of Medicine and Health Sciences, Norwegian University of  
571 Science and Technology (NTNU). The genotype quality control and imputation has been  
572 conducted by the K.G. Jebsen center for genetic epidemiology, Department of public health and  
573 nursing, Faculty of medicine and health sciences, Norwegian University of Science and  
574 Technology (NTNU).

575 **CONTRIBUTIONS**

576 SK, MP and LD designed the study and wrote the manuscript. SK and MP performed analyses.  
577 The HUNT group provided summary GWAS data for replication. EVP, MR, ST performed the  
578 imaging analysis. JM, AK contributed to result interpretation. All the authors read and edited the  
579 final manuscript.

580 HUNT All-In Pain

581 Anne Heidi Skogholt<sup>1</sup>

582 Ben Brumpton<sup>1</sup>

583 Cristen J. Willer<sup>2</sup>

584 Egil Andreas Fors<sup>3</sup>

585 Ingrid Heuch<sup>4</sup>

586 Jonas Bille Nielsen<sup>1,2,5</sup>

587 Kjersti Storheim<sup>6,7</sup>

588 Knut Hagen<sup>8</sup>

589 Kristian Bernhard Nilsen<sup>8,9</sup>

590 Kristian Hveem<sup>1,10,11</sup>  
591 Lars Fritsche<sup>12</sup>  
592 Laurent F. Thomas<sup>1,13,14,15</sup>  
593 Linda M Pedersen<sup>4</sup>  
594 Maiken E Gabrielsen<sup>1</sup>  
595 Marianne Bakke Johnsen<sup>1,6,16</sup>  
596 Marie Udneseter Lie<sup>6,16</sup>  
597 Oddgeir Holmen<sup>10</sup>  
598 Sigrid Børte<sup>1,6,16</sup>  
599 Synne Øien Stensland<sup>6,17</sup>  
600 Wei Zhou<sup>18,19</sup>

601  
602

603 1 K. G. Jebsen Center for Genetic Epidemiology, Department of Public Health and Nursing, Faculty of Medicine  
604 and Health Sciences, Norwegian University of Science and Technology, Trondheim, Norway.

605 2 Department of Internal Medicine, Division of Cardiovascular Medicine, University of Michigan, Ann Arbor,  
606 48109, MI, USA.

607 3 Department of Public Health and Nursing, Faculty of Medicine and Health Sciences, Norwegian University of  
608 Science and Technology, Trondheim, Norway.

609 4 Department of Research, Innovation and Education, Division of Clinical Neuroscience, Oslo University Hospital,  
610 Oslo, Norway.

611 5 Department of Epidemiology Research, Statens Serum Institut, Copenhagen, Denmark.

612 6 Research and Communication Unit for Musculoskeletal Health (FORMI), Department of Research, Innovation and  
613 Education, Division of Clinical Neuroscience, Oslo University Hospital, Oslo, Norway.

614 7 Faculty of Health Sciences, Department of physiotherapy, Oslo Metropolitan University, Oslo, Norway.

615 8 Department of Neuromedicine and Movement Science, Faculty of Medicine and Health Sciences, Norwegian  
616 University of Science and Technology (NTNU), Trondheim, Norway.

617 9 Department of Neurology, Oslo University Hospital, Oslo, Norway.

618 10 HUNT Research Center, Department of Public Health and Nursing, Faculty of Medicine and Health Sciences,  
619 Norwegian University of Science and Technology, Trondheim, Norway.

620 11 Department of Research, Innovation and Education, St. Olavs Hospital, Trondheim University Hospital,  
621 Trondheim, Norway.

622 12 Center for Statistical Genetics, Department of Biostatistics, University of Michigan, Ann Arbor, 48109, MI,  
623 USA.

624 13 Department of Clinical and Molecular Medicine, Norwegian University of Science and Technology, Trondheim,  
625 Norway.

626 14 BioCore - Bioinformatics Core Facility, Norwegian University of Science and Technology, Trondheim, Norway.

627 15 Clinic of Laboratory Medicine, St.Olavs Hospital, Trondheim University Hospital, Trondheim, Norway.

628 16 Institute of Clinical Medicine, Faculty of Medicine, University of Oslo, Oslo, Norway.

629 17 NKVTS, Norwegian Centre for Violence and Traumatic Stress Studies.

630 18 Department of Computational Medicine and Bioinformatics, University of Michigan, Ann Arbor, MI, USA.

631 19 Analytic and Translational Genetics Unit, Massachusetts General Hospital, Boston, Massachusetts, USA.

632  
633

## 634 **COMPETING INTERESTS STATEMENT**

635 The authors declare no competing financial interests.

636

637 **FIGURE LEGENDS AND TABLES**

638 **Figure 1.** Pain sites characteristics and correlations in UK Biobank **(A)** Pain sites mapped to the  
639 human body. Black dots indicate the sites in the front of the body, while grey dots indicate the  
640 sites in the back of the body. Number of cases at each site shown in parenthesis. Human body  
641 image from clipart-library.com. **(B)** Epidemiologic and genetic correlations between pain sites.  
642 Heatmap showing correlations for co-occurrence of pain sites. Correlations at the epidemiologic  
643 odds ratios (OR) are shown in purple hues, while genetic odds ratios (Rg) are shown in orange  
644 hues. Grey cells indicate statistical non-significance after Bonferroni correction for the number  
645 of same-colored cells. **(C)** Scatterplot showing correlation between epidemiologic OR and body  
646 map distance. Each dot is a pair of pain sites out of a total of 21. Also shown are percent variance  
647 explained ( $r^2$ ), slope of regression ( $m$ ), and associated  $P$ -value ( $P$ ). **(D)** Scatterplot showing  
648 correlation between genetic Rg and body map distance. **(E)** Scatterplot showing correlation  
649 between genetic Rg and epidemiologic OR. **(F)** Narrow-sense heritability estimates for each pain  
650 site (blue), for chronic single-site pain (orange), and for chronic multi-site pain (brown). 95%  
651 CIs shown in black. The difference in heritability is highly significant (\*\*\*)  $P < 2.2 \times 10^{-16}$ .

652 **Figure 2.** Genome-wide association studies for single-site pain and multi-site pain. Shown are  
653 Manhattan plots at the SNP-level (top) and at the gene-level (bottom). SNP  $P$ -values are  
654 obtained from BOLT or GWAMA, while gene  $P$ -values are obtained from MAGMA.  
655 Alternating dark and light color hues used for odd and even chromosome numbers. Genome-  
656 wide significance highlighted by a horizontal red line at SNP-level is from Bonferroni's  
657 threshold of  $5 \times 10^{-8}$ , while at gene-level is at FDR 1%. **(A)** Single-vs-no chronic pain site. **(B)**  
658 Multi-site-vs-no chronic pain sites. **(C)** Unique loci derived from a meta-analysis in GWAMA.  
659 **(D)** Pleiotropic loci from a meta-analysis in GWAMA.

660 **Figure 3.** Partitioned heritability for single-site pain and multi-site pain. **(A)** Seventy-eight  
661 tissues were grouped into eight tissue classes: central nervous system (CNS, green,  $n=21$ ),  
662 peripheral nervous system (PNS, blue,  $n=4$ ), endocrine (END, purple,  $n=2$ ), myeloid (MYE, red,  
663  $n=16$ ), B cells (B, orange,  $n=8$ ) T cells (T, purple,  $n=22$ ), adipose (ADI, brown,  $n=2$ ) and muscle  
664 (MUS, grey,  $n=3$ ). Shown for each tissue is  $-\log_{10}$  of FDR-adjusted  $P$ -value for enrichment.  
665 Heritability estimated for single-site pain (top) and for multi-pain sites are shown (COPC;  
666 bottom). Statistical threshold of significance is highlighted at the FDR 10% level with horizontal  
667 red lines, while significant tissues with colored filled boxes. **(B)** Zoom into the CNS tissues for  
668 multi-site pain. **(C)** Scatter plot of heritability coefficients in single-site pain versus multi-site  
669 pain. Each dot is a tissue of the CNS. Orange line obtained from linear regression, with percent  
670 variance explained ( $r^2$ ), slope ( $m$ ) and regression  $P$ -value ( $P$ ) shown.

671 **Figure 4.** Functional validation for a role of *DCC* in the human brain. **(A)** Whole brain  
672 expression of *DCC* computed from the Allen Brain Atlas. **(B)** Zoom into the expression of *DCC*  
673 in the subcortical limbic regions. **(C)** Representation of the uncinate fasciculus (UF) white matter  
674 tract. **(D)** Bar plot of bilateral dispersion orientation (OD) of the UF in the no-pain controls,  
675 single-site pain, multi-site pain states. The y-axis represents OD values for the UF. Bars  
676 represent standard error.  $*P<0.05$ ;  $***P<0.0001$ . **(E)** Polygenic risk score (PRS) generated using  
677 PRSice from summary GWAS of single-site pain, multi-site pain, axonogenesis pathway, and  
678 *DCC*. Plotted is the  $-\log_{10}$   $P$ -value of the regression model using PRS with the score selected at  
679 the best fit  $P$ -value threshold.

680 **Table 1.** Demographic and phenotypic characteristics of the study population.

681 **Table 2.** Replication of results on multi-site pain from UK Biobank in HUNT.

682

683 **SUPPLEMENTARY MATERIALS**

684 **Supplementary Figure 1.** Histogram of number of UK Biobank participants per reported  
685 number of chronic pain sites.

686 **Supplementary Figure 2.** QQ plot: Quantile-quantile plot shows the observed versus expected –  
687  $\log_{10}$  p-values from A) one pain site and B) multi-site pain association analysis.

688 **Supplementary Figure 3.** Locus Zoom plots for each of the 23 genome-wide significant loci.

689 **Supplementary Table 1.** Prevalence of acute and chronic pain sites in UK Biobank.

690 **Supplementary Table 2.** Epidemiological odds of reporting pairs of chronic pain sites.

691 **Supplementary Table 3.** Genetic correlation between pairs of chronic pain sites.

692 **Supplementary Table 4.** Latent causal variable analysis between chronic pain sites.

693 **Supplementary Table 5.** Heritability estimates for chronic pain sites.

694 **Supplementary Table 6.** List of top SNPs associated with single-site pain.

695 **Supplementary Table 7.** List of protein-coding genes associated with single-site pain.

696 **Supplementary Table 8.** List of genome-wide loci associated with multi-site pain.

697 **Supplementary Table 9.** List of protein-coding genes associated with multi-site pain.

698 **Supplementary Table 10.** List of protein-coding genes derived from GWAMA that are unique  
699 for single-site pain or multi-site pain GWASs.

700 **Supplementary Table 11.** List of protein-coding genes derived from GWAMA that are  
701 pleiotropic between single-site pain or multi-site pain GWASs.

702 **Supplementary Table 12.** Tissue-specific partitioned heritability within the Xavier lab dataset  
703 for single-site pain.

704 **Supplementary Table 13.** Tissue-specific partitioned heritability within the Xavier lab dataset  
705 for multi-site pain.



706 **Supplementary Table 14.** Pathway-based functional analyses for single-site pain GWAS. **(A)**  
707 Analysis in Gene Ontology's biological processes.

708 **Supplementary Table 15.** Pathway-based functional analyses for multi-site pain GWAS. **(A)**  
709 Analysis in Gene Ontology's biological processes. **(B)** Reduced pathway sets from revigo.

710 **Supplementary Table 16.** Replication in HUNT cohort. **(A)** Locus-level; **(B)** Gene-level; **(C)**  
711 Pathway level.

712 **Supplementary Table 17.** Polygenic risk score (PRS) regression models testing left, right, and  
713 bilateral orientation dispersion of the uncinatus fasciculus (UF).  
714

## 715 REFERENCES

- 716 1. Fayaz, A., Croft, P., Langford, R.M., Donaldson, L.J. & Jones, G.T. Prevalence of chronic pain in  
717 the UK: a systematic review and meta-analysis of population studies. *BMJ Open* **6**, e010364  
718 (2016).
- 719 2. Shupler, M.S., Kramer, J.K., Cragg, J.J., Jutzeler, C.R. & Whitehurst, D.G.T. Pan-Canadian  
720 estimates of chronic pain prevalence from 2000 to 2014: A Repeated Cross-Sectional Survey  
721 Analysis. *J Pain* (2018).
- 722 3. Schopflocher, D., Taenzer, P. & Jovey, R. The prevalence of chronic pain in Canada. *Pain Res*  
723 *Manag* **16**, 445-50 (2011).
- 724 4. Page, M.G., Fortier, M., Ware, M.A. & Choiniere, M. As if one pain problem was not enough:  
725 prevalence and patterns of coexisting chronic pain conditions and their impact on treatment  
726 outcomes. *J Pain Res* **11**, 237-254 (2018).
- 727 5. Maixner, W., Fillingim, R.B., Williams, D.A., Smith, S.B. & Slade, G.D. Overlapping Chronic  
728 Pain Conditions: Implications for Diagnosis and Classification. *J Pain* **17**, T93-t107 (2016).
- 729 6. Larkin, T.E. *et al.* Altered network architecture of functional brain communities in chronic  
730 nociplastic pain. *Neuroimage* **226**, 117504 (2021).
- 731 7. Schrepf, A. *et al.* ICD-10 Codes for the Study of Chronic Overlapping Pain Conditions in  
732 Administrative Databases. *J Pain* **21**, 59-70 (2020).
- 733 8. Nielsen, C.S., Knudsen, G.P. & Steingrimsdottir, O.A. Twin studies of pain. *Clin Genet* **82**, 331-  
734 40 (2012).
- 735 9. Vehof, J., Zavos, H.M., Lachance, G., Hammond, C.J. & Williams, F.M. Shared genetic factors  
736 underlie chronic pain syndromes. *Pain* **155**, 1562-8 (2014).
- 737 10. Gasperi, M. *et al.* Chronic prostatitis and comorbid non-urological overlapping pain conditions: A  
738 co-twin control study. *J Psychosom Res* **102**, 29-33 (2017).
- 739 11. Meloto, C.B. *et al.* Human pain genetics database: a resource dedicated to human pain genetics  
740 research. *Pain* **159**, 749-763 (2018).
- 741 12. Suri, P. *et al.* Genome-wide meta-analysis of 158,000 individuals of European ancestry identifies  
742 three loci associated with chronic back pain. *PLoS Genet* **14**, e1007601 (2018).
- 743 13. Johnston, K.J.A. *et al.* Genome-wide association study of multisite chronic pain in UK Biobank.  
744 *PLoS Genet* **15**, e1008164 (2019).
- 745 14. Kennedy, T.E., Serafini, T., de la Torre, J.R. & Tessier-Lavigne, M. Netrins are diffusible  
746 chemotropic factors for commissural axons in the embryonic spinal cord. *Cell* **78**, 425-35 (1994).
- 747 15. Yamagata, M., Weiner, J.A. & Sanes, J.R. Sidekicks: synaptic adhesion molecules that promote  
748 lamina-specific connectivity in the retina. *Cell* **110**, 649-60 (2002).
- 749 16. Mägi, R. & Morris, A.P. GWAMA: software for genome-wide association meta-analysis. *BMC*  
750 *Bioinformatics* **11**, 288 (2010).
- 751 17. Finucane, H.K. *et al.* Partitioning heritability by functional annotation using genome-wide  
752 association summary statistics. *Nat Genet* **47**, 1228-35 (2015).
- 753 18. Finucane, H.K. *et al.* Heritability enrichment of specifically expressed genes identifies disease-  
754 relevant tissues and cell types. *Nat Genet* **50**, 621-629 (2018).
- 755 19. Benita, Y. *et al.* Gene enrichment profiles reveal T-cell development, differentiation, and lineage-  
756 specific transcription factors including ZBTB25 as a novel NF-AT repressor. *Blood* **115**, 5376-84  
757 (2010).
- 758 20. Fehrmann, R.S. *et al.* Gene expression analysis identifies global gene dosage sensitivity in cancer.  
759 *Nat Genet* **47**, 115-25 (2015).
- 760 21. Supek, F., Bosnjak, M., Skunca, N. & Smuc, T. REVIGO summarizes and visualizes long lists of  
761 gene ontology terms. *PLoS One* **6**, e21800 (2011).
- 762 22. Hawrylycz, M.J. *et al.* An anatomically comprehensive atlas of the adult human brain  
763 transcriptome. *Nature* **489**, 391-399 (2012).

- 764 23. Aaron, L.A., Burke, M.M. & Buchwald, D. Overlapping conditions among patients with chronic  
765 fatigue syndrome, fibromyalgia, and temporomandibular disorder. *Arch Intern Med* **160**, 221-7  
766 (2000).
- 767 24. Nickel, J.C. *et al.* Interstitial cystitis/painful bladder syndrome and associated medical conditions  
768 with an emphasis on irritable bowel syndrome, fibromyalgia and chronic fatigue syndrome. *J*  
769 *Urol* **184**, 1358-63 (2010).
- 770 25. Schafer, I. *et al.* Reducing complexity: a visualisation of multimorbidity by combining disease  
771 clusters and triads. *BMC Public Health* **14**, 1285 (2014).
- 772 26. Gormley, P. *et al.* Meta-analysis of 375,000 individuals identifies 38 susceptibility loci for  
773 migraine. *Nat Genet* **48**, 856-66 (2016).
- 774 27. Zorina-Lichtenwalter, K., Meloto, C.B., Khoury, S. & Diatchenko, L. Genetic predictors of  
775 human chronic pain conditions. *Neuroscience* **338**, 36-62 (2016).
- 776 28. Meng, W. *et al.* A Genome-Wide Association Study Finds Genetic Associations with Broadly-  
777 Defined Headache in UK Biobank (N=223,773). *EBioMedicine* **28**, 180-186 (2018).
- 778 29. Glasgow, S.D. *et al.* Activity-Dependent Netrin-1 Secretion Drives Synaptic Insertion of GluA1-  
779 Containing AMPA Receptors in the Hippocampus. *Cell Rep* **25**, 168-182 e6 (2018).
- 780 30. Wu, C.H. *et al.* Netrin-1 Contributes to Myelinated Afferent Fiber Sprouting and Neuropathic  
781 Pain. *Mol Neurobiol* **53**, 5640-51 (2016).
- 782 31. Serafini, T. *et al.* The netrins define a family of axon outgrowth-promoting proteins homologous  
783 to *C. elegans* UNC-6. *Cell* **78**, 409-24 (1994).
- 784 32. Keino-Masu, K. *et al.* Deleted in Colorectal Cancer (DCC) encodes a netrin receptor. *Cell* **87**,  
785 175-85 (1996).
- 786 33. da Silva, R.V. *et al.* DCC Is Required for the Development of Nociceptive Topognosis in Mice  
787 and Humans. *Cell Rep* **22**, 1105-1114 (2018).
- 788 34. Schubert, A.L., Held, M., Sommer, C. & Üçeyler, N. Reduced gene expression of netrin family  
789 members in skin and sural nerve specimens of patients with painful peripheral neuropathies. *J*  
790 *Neurol* **266**, 2812-2820 (2019).
- 791 35. Olson, I.R., Von Der Heide, R.J., Alm, K.H. & Vyas, G. Development of the uncinat fasciculus:  
792 Implications for theory and developmental disorders. *Dev Cogn Neurosci* **14**, 50-61 (2015).
- 793 36. Manitt, C. *et al.* dcc orchestrates the development of the prefrontal cortex during adolescence and  
794 is altered in psychiatric patients. *Transl Psychiatry* **3**, e338 (2013).
- 795 37. Wu, Y. *et al.* Multi-trait analysis for genome-wide association study of five psychiatric disorders.  
796 *Transl Psychiatry* **10**, 209 (2020).
- 797 38. Ward, J. *et al.* Genome-wide analysis in UK Biobank identifies four loci associated with mood  
798 instability and genetic correlation with major depressive disorder, anxiety disorder and  
799 schizophrenia. *Transl Psychiatry* **7**, 1264 (2017).
- 800 39. Yang, Q., Wang, Z., Yang, L., Xu, Y. & Chen, L.M. Cortical thickness and functional  
801 connectivity abnormality in chronic headache and low back pain patients. *Hum Brain Mapp* **38**,  
802 1815-1832 (2017).
- 803 40. Allen, N.E., Sudlow, C., Peakman, T., Collins, R. & Biobank, U.K. UK biobank data: come and  
804 get it. *Sci Transl Med* **6**, 224ed4 (2014).
- 805 41. Sudlow, C. *et al.* UK biobank: an open access resource for identifying the causes of a wide range  
806 of complex diseases of middle and old age. *PLoS Med* **12**, e1001779 (2015).
- 807 42. Loh, P.R. *et al.* Efficient Bayesian mixed-model analysis increases association power in large  
808 cohorts. *Nat Genet* **47**, 284-90 (2015).
- 809 43. Bulik-Sullivan, B.K. *et al.* LD Score regression distinguishes confounding from polygenicity in  
810 genome-wide association studies. *Nat Genet* **47**, 291-5 (2015).
- 811 44. Bulik-Sullivan, B. *et al.* An atlas of genetic correlations across human diseases and traits. *Nat*  
812 *Genet* **47**, 1236-41 (2015).
- 813 45. Magi, R., Lindgren, C.M. & Morris, A.P. Meta-analysis of sex-specific genome-wide association  
814 studies. *Genet Epidemiol* **34**, 846-53 (2010).

- 815 46. Watanabe, K., Taskesen, E., van Bochoven, A. & Posthuma, D. Functional mapping and  
816 annotation of genetic associations with FUMA. *Nature Communications* **8**, 1826 (2017).
- 817 47. de Leeuw, C.A., Mooij, J.M., Heskes, T. & Posthuma, D. MAGMA: generalized gene-set  
818 analysis of GWAS data. *PLoS Comput Biol* **11**, e1004219 (2015).
- 819 48. The\_Gene\_Ontology\_Consortium. The Gene Ontology Resource: 20 years and still GOing  
820 strong. *Nucleic Acids Res* **47**, D330-D338 (2019).
- 821 49. Holmen, T.L. *et al.* Cohort profile of the Young-HUNT Study, Norway: a population-based study  
822 of adolescents. *Int J Epidemiol* **43**, 536-44 (2014).
- 823 50. Krokstad, S. *et al.* Cohort Profile: the HUNT Study, Norway. *Int J Epidemiol* **42**, 968-77 (2013).
- 824 51. Hagen, K., Linde, M., Heuch, I., Stovner, L.J. & Zwart, J.A. Increasing prevalence of chronic  
825 musculoskeletal complaints. A large 11-year follow-up in the general population (HUNT 2 and  
826 3). *Pain Med* **12**, 1657-66 (2011).
- 827 52. Jun, G. *et al.* Detecting and estimating contamination of human DNA samples in sequencing and  
828 array-based genotype data. *Am J Hum Genet* **91**, 839-48 (2012).
- 829 53. Guo, Y. *et al.* Illumina human exome genotyping array clustering and quality control. *Nat Protoc*  
830 **9**, 2643-62 (2014).
- 831 54. Consortium, E.P. An integrated encyclopedia of DNA elements in the human genome. *Nature*  
832 **489**, 57-74 (2012).
- 833 55. Wang, C. *et al.* Ancestry estimation and control of population stratification for sequence-based  
834 association studies. *Nat Genet* **46**, 409-15 (2014).
- 835 56. Li, J.Z. *et al.* Worldwide human relationships inferred from genome-wide patterns of variation.  
836 *Science* **319**, 1100-4 (2008).
- 837 57. Loh, P.R. *et al.* Reference-based phasing using the Haplotype Reference Consortium panel. *Nat*  
838 *Genet* **48**, 1443-1448 (2016).
- 839 58. Das, S. *et al.* Next-generation genotype imputation service and methods. *Nat Genet* **48**, 1284-  
840 1287 (2016).
- 841 59. McCarthy, S. *et al.* A reference panel of 64,976 haplotypes for genotype imputation. *Nat Genet*  
842 **48**, 1279-83 (2016).
- 843 60. Zhou, W. *et al.* Efficiently controlling for case-control imbalance and sample relatedness in large-  
844 scale genetic association studies. *Nat Genet* **50**, 1335-1341 (2018).
- 845 61. Chang, C.C. *et al.* Second-generation PLINK: rising to the challenge of larger and richer datasets.  
846 *Gigascience* **4**, 7 (2015).
- 847 62. Xian, M., Wang, J. & He, Y. BrainNet Viewer: A Network Visualization Tool for Human Brain  
848 Connectomics. *Plos One* **8**, e68910 (2013).
- 849 63. Choi, S.W. & O'Reilly, P.F. PRSice-2: Polygenic Risk Score software for biobank-scale data.  
850 *GigaScience* **8**(2019).
- 851

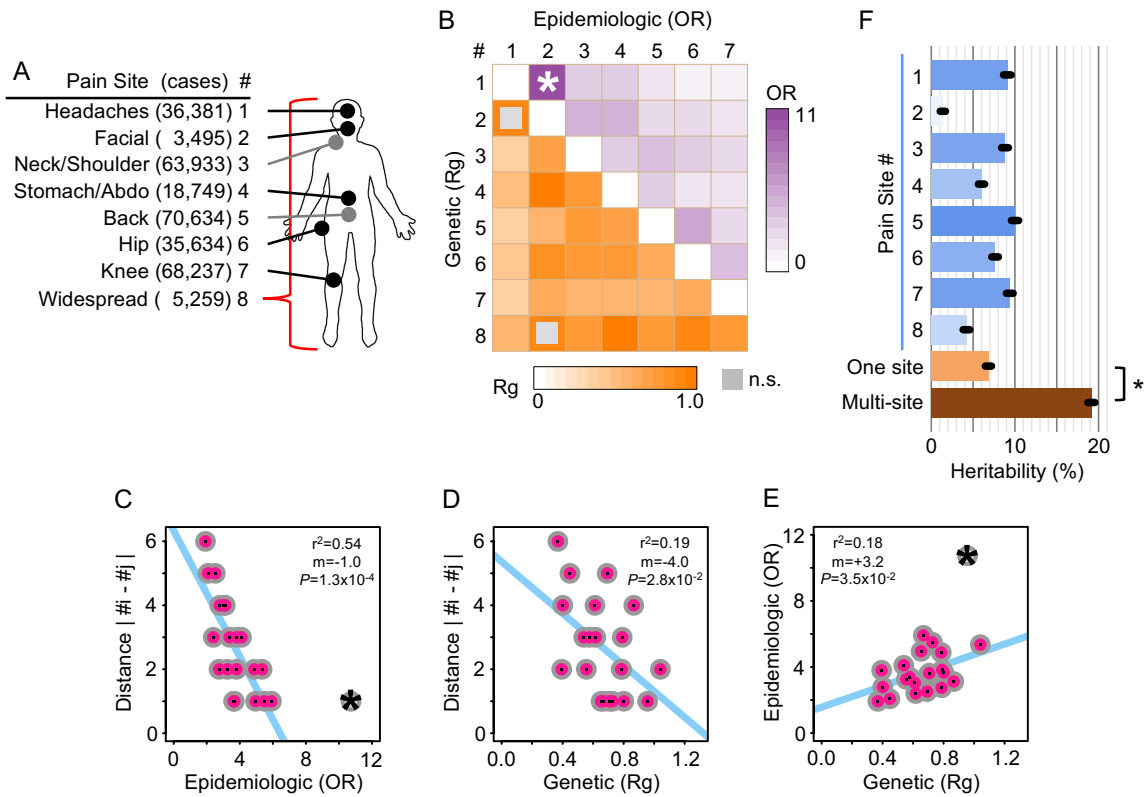


**Figure 1.** Pain sites characteristics and correlations in UK biobank **(A)** Pain sites mapped to the human body. Black dots indicate the sites in the front of the body, while grey dots indicate the sites in the back of the body. Number of cases at each site shown in parenthesis. Human body image from clipart-library.com. **(B)** Epidemiologic and genetic correlations between pain sites. Heatmap showing correlations for co-occurrence of pain sites. Correlations at the epidemiologic odds ratios (OR) are shown in purple hues, while genetic odds ratios (Rg) are shown in orange hues. Grey cells indicate statistical non-significance after Bonferroni correction for the number of same-colored cells. **(C)** Scatter plot showing correlation between epidemiologic OR and body map distance. Each dot is a pair of pain sites out of a total of 21. Also shown are percent variance explained ( $r^2$ ), slope of regression ( $m$ ), and associated P-value ( $P$ ). **(D)** Scatter plot showing correlation between genetic Rg and body map distance. **(E)** Scatter plot showing correlation between genetic Rg and epidemiologic OR. **(F)** Narrow-sense heritability estimates for each pain site (blue), for chronic single-site pain (orange), and for chronic multi-site pain (brown). 95% confidence intervals shown in black. The difference in heritability is highly significant ( $*** P < 2.2 \times 10^{-16}$ ).

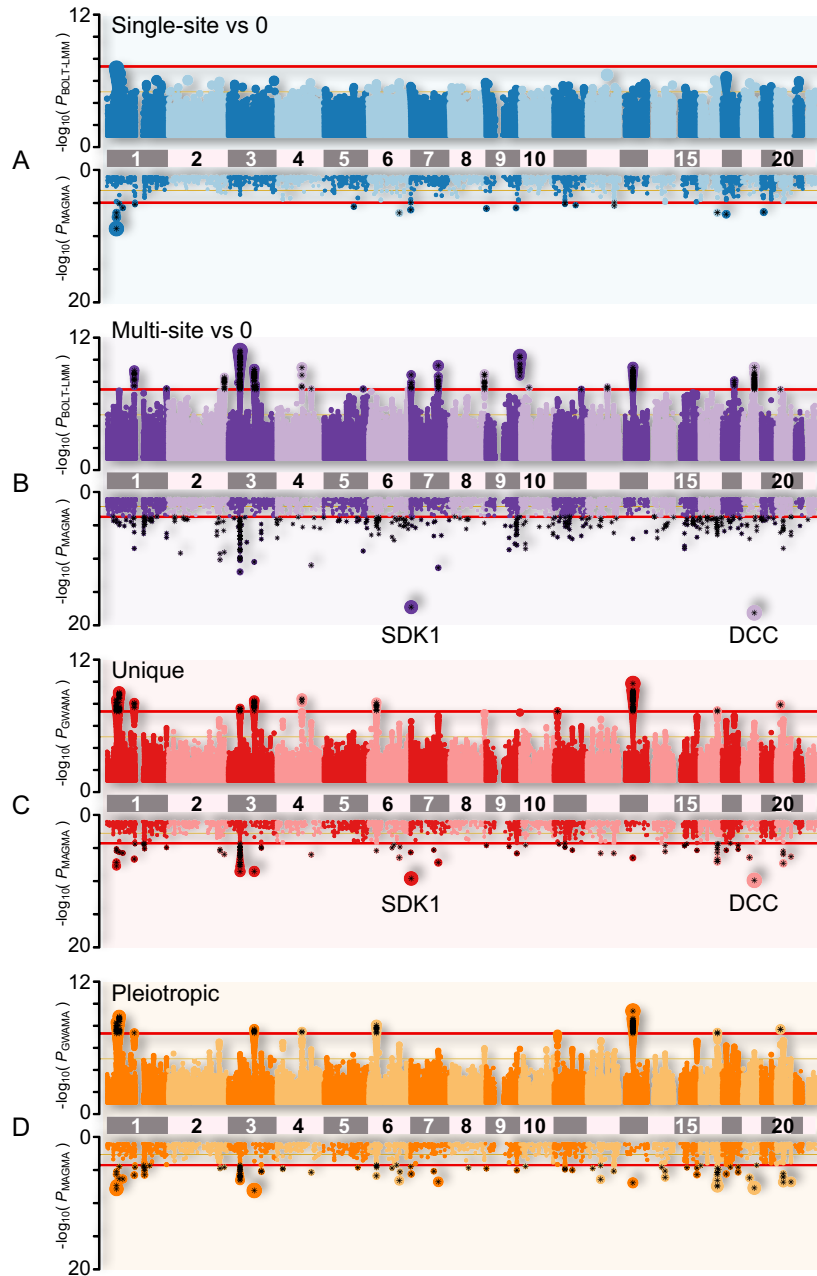


**Figure 2.** Genome-wide association studies for single-site pain and multi-site pain. Shown are Manhattan plots at the SNP-level (top) and at the gene-level (bottom). SNP P-values are obtained from BOLT or GWAMA, while gene P-values are obtained from MAGMA. Alternating dark and light color hues used for odd and even chromosome numbers. Genome-wide significance highlighted by a horizontal red line at SNP-level is from Bonferroni's threshold of  $5 \times 10^{-8}$ , while at gene-level is at FDR 1%. **(A)** Single-site-vs-no chronic pain site. **(B)** Multi-site-vs-no chronic pain sites. **(C)** Unique loci derived from a meta-analysis in GWAMA. **(D)** Pleiotropic loci from a meta-analysis in GWAMA.

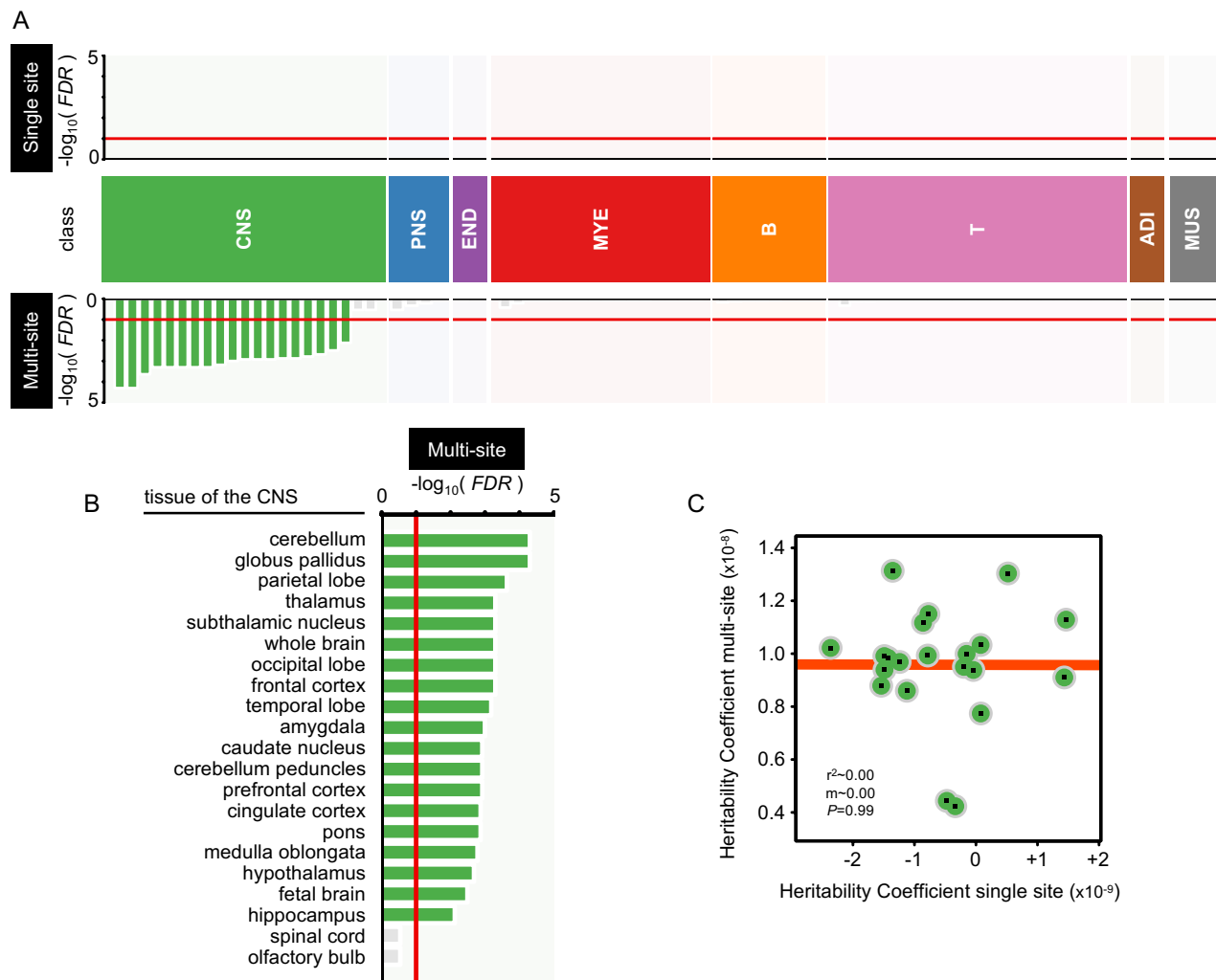


**Figure 3.** Partitioned heritability for single-site pain and multi-site pain. **(A)** Seventy-eight tissues were grouped into eight tissue classes: central nervous system (CNS, green,  $n=21$ ), peripheral nervous system (PNS, blue,  $n=4$ ), endocrine (END, purple,  $n=2$ ), myeloid (MYE, red,  $n=16$ ), B cells (B, orange,  $n=8$ ) T cells (T, purple,  $n=22$ ), adipose (ADI, brown,  $n=2$ ) and muscle (MUS, grey,  $n=3$ ). Shown for each tissue is  $-\log_{10}$  of FDR-adjusted P-value for enrichment. Heritability estimated for single-site pain (top) and for multi-pain sites are shown (COPC; bottom). Statistical threshold of significance is highlighted at the FDR 10% level with horizontal red lines, while significant tissues with colored filled boxes. **(B)** Zoom into the central nervous system tissues for multi-site pain. **(C)** Scatter plot of heritability coefficients in single-site pain versus multi-site pain. Each dot is a tissue of the CNS. Orange line obtained from linear regression, with percent variance explained ( $r^2$ ), slope ( $m$ ) and regression P-value ( $P$ ) shown.

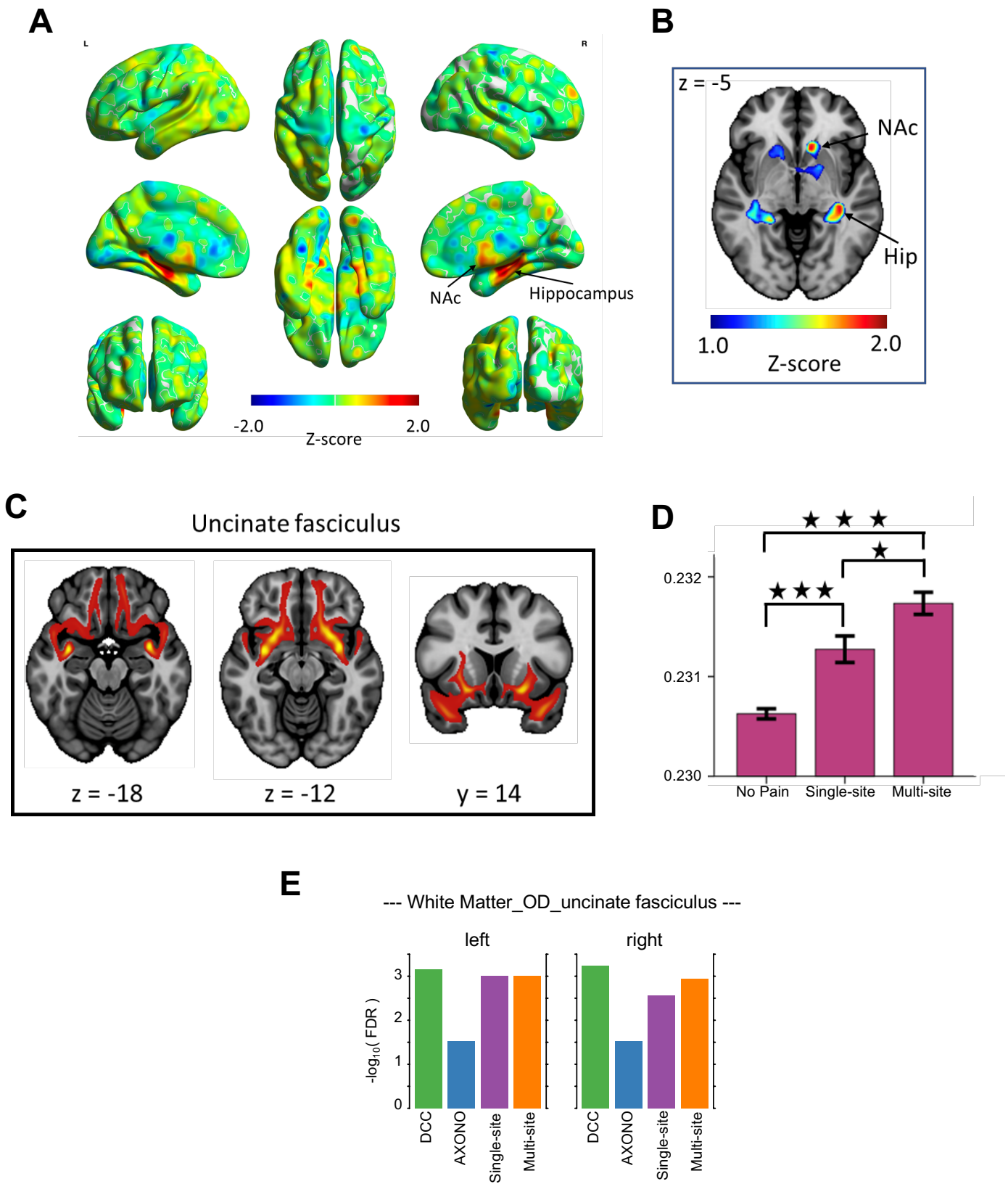


**Figure 4.** Functional validation for a role of DCC in the human brain (A) Whole brain expression of DCC computed from the Allen Brain Atlas (B) Zoom into the expression of DCC in the subcortical limbic regions (C) Representation of the uncinate fasciculus (UF) white matter tract (D) Bar plot of bilateral dispersion orientation (OD) of the UF in the no-pain controls, single-site pain, multi-site pain states. The Y-axis represents OD values for the UF. Bars represent standard error. \*\*\* $p < 0.0001$ ; \* $p = 0.02$  (E) Polygenic risk score generated using PRSice from summary GWAS of single-site pain, multi-site pain, axonogenesis pathway, and DCC. Plotted is the  $-\log_{10}$  p-value of the regression model using PRS with the score selected at the best fit p-value threshold.



Table 1 – Demographic and phenotypic characteristics of study population

	Controls	One-site	Multi-site	P-value
Females (%)	52.4%	54.2%	60.7%	<0.0001
Age (mean)	56.78	56.67	56.98	<0.0001
BMI (mean)	26.70	27.67	28.66	<0.0001
Smoking status (current)	8.8%	10.8%	13.6%	<0.0001
Townsend deprivation index (mean)	-1.60	-1.32	-0.80	<0.0001
Number of self-reported cancers	0.09	0.09	0.1	<0.0001
Number of self-reported non-cancer illnesses	1.44	1.94	2.83	<0.0001
Medication for pain relief				
Paracetamol (n)	20,846	28,800	40,954	<0.0001
Ibuprofen (n)	14,480	21,137	24,468	<0.0001
Aspirin (n)	23,418	16,278	17,602	<0.0001
Depressed mood last two weeks				<0.0001
Severe days	12.9%	18.9%	25.6%	
More than half the days	1.6%	3.0%	5.5%	
Nearly every day	0.9%	1.7%	4.4%	
Number of depression episodes (mean)	2.44	2.78	3.21	<0.0001
Neuroticism score (mean)	3.35	4.32	5.41	<0.0001

Categorical data were compared using a chi-square test and quantitative data are compared using a t-test. The overall p-value is an ANOVA between the three groups.

Table 2 – Replication of multi-site chronic pain results from UK biobank in HUNT

a) Loci SNP level

Loci	Lead SNP	Genes in locus	HUNT p-value
Chr3 :49,206,000-49,891,000	rs11709734	<i>APEH, BSN, C3orf62, C3orf84, CCDC36, CDHR4, DGA1, GMPPB, GPX1, IP6K1, KLHDC81B, MST1, MST1R, NICN1, RHOA, RNF123, TCTA, TRAIP, UBA7, USP4</i>	rs184219667 ( $r^2=0.96$ ) $1.36 \times 10^{-3}$
Chr4 :140,600,000-141,000,000	rs34595097	<i>MAML3</i>	rs1204594 ( $r^2=0.54$ ) $2.33 \times 10^{-4}$
Ch7 :113,770,000-114,267,000	rs12672683	<i>FOXP2</i>	rs62469212 ( $r^2=0.51$ ) $1.42 \times 10^{-3}$
Chr18 : 50,073,000-50,908,000	rs8099145	<i>DCC</i>	rs17410557 ( $r^2=0.58$ ) $1.68 \times 10^{-4}$

b) Gene level

HUGO	CHR	START	STOP	Z stat	HUNT P-value	FDR	
<i>DCC</i>	18	49866542	51062273	5.44	2.64E-08	0.000497	DCC netrin 1 receptor
<i>CAMKV</i>	3	49895414	49907655	4.10	2.00E-05	0.047772	CaM Kinase like vesicle associated
<i>IP6K1</i>	3	49761728	49823973	4.10	2.03E-05	0.047772	Inositol hexakisphosphate kinase 1
<i>MONIA</i>	3	49946302	49967445	4.01	3.09E-05	0.058253	MON1 homolog A, secretory trafficking associated
<i>MAML3</i>	4	1.41E+08	1.41E+08	3.90	4.82E-05	0.070071	Mastermind like transcriptional coactivator 3
<i>RNF123</i>	3	49726950	49758962	3.68	0.000119	0.083047	Ring finger protein 123
<i>ZBTB46</i>	20	62375021	62463731	3.53	0.000209	0.108017	Zinc finger and BTB Domain containing 46
<i>BSN</i>	3	49591922	49708982	3.45	0.000284	0.118353	Bassoon presynaptic cytomatrix protein
<i>TRAIP</i>	3	49866028	49893992	3.38	0.000357	0.126412	TRAF interacting protein
<i>RBM6</i>	3	49977474	50114685	3.32	0.000454	0.144758	RNA binding motif protein 6
<i>MST1</i>	3	49721380	49726196	3.26	0.00056	0.159801	Macrophage stimulating 1

c) Pathway level

<b>VARIABLE</b>	<b>DESC</b>	<b>HUNT P-value</b>	<b>FDR</b>
GO:0007409	axonogenesis	0.00095495	0.547171
GO:0061564	axon development	0.0013778	0.547171
GO:0042297	vocal learning	0.0014606	0.547171
GO:0098596	imitative learning	0.0014606	0.547171
GO:0048812	neuron projection morphogenesis	0.0023204	0.595695
GO:0048667	cell morphogenesis involved in neuron differentiation	0.0023438	0.595695
GO:0120039	plasma membrane bounded cell projection morphogenesis	0.0024645	0.595695
GO:0048858	cell projection morphogenesis	0.0026534	0.595695
GO:0006206	pyrimidine nucleobase metabolic process	0.0036173	0.612315
GO:0098597	observational learning	0.0040134	0.612315
GO:0032913	negative regulation of transforming growth factor beta3 production	0.0040365	0.612315
GO:0007638	mechanosensory behavior	0.0058522	0.621343
GO:0032990	cell part morphogenesis	0.0058527	0.621343
GO:0098598	learned vocalization behavior or vocal learning	0.0059061	0.621343
GO:0010608	posttranscriptional regulation of gene expression	0.0069535	0.63441
GO:0031223	auditory behavior	0.0069601	0.63441
GO:0030182	neuron differentiation	0.0099669	0.690212
GO:0007399	nervous system development	0.03211	0.773552
GO:0022008	neurogenesis	0.033344	0.773786
GO:0071625	vocalization behavior	0.03577	0.778559
GO:0048468	cell development	0.038141	0.78672
GO:0010468	regulation of gene expression	0.042054	0.78672
GO:0000904	cell morphogenesis involved in differentiation	0.044285	0.78672
GO:0006208	pyrimidine nucleobase catabolic process	0.047884	0.78672